Electronic Supplementary Material (ESI) for Dalton Transactions

Supporting Information for:

Tuning the interactions from antiferro- to ferro-magnetic by molecular tailoring and manipulating

Xiaoying Zhang,[a] Bo Li,[a, b] Jinkui Tang,[c] Jumei Tian,[a] Guolong Huang,[a] and Jingping Zhang,*[,a]

[a] *Faculty of Chemistry, Northeast Normal University, Changchun 130024, P. R. China*.

[b] *Hebei Provincial Key Laboratory of Inorganic Nonmetallic Materials, College of Materials Science and Engineering, Hebei United University, Hebei, Tangshan 063009, China.*

[c] *Changchun Institute of Applied Chemistry, Chinese Academy of Sciences, Changchun 130022, China.*

1. X-ray Crystallography. Single-crystal X-ray data sets of complexes **1-4** were collected on a Oxford Diffraction Gemini R Ultra detector diffractometer using the graphite monochromated Mo Kα radiation (λ = 0.71073 Å) at 298(2) K but 185(2) K for **1** and **3**. Intense data were collected by ω scan technique. The diffraction patterns for both complexes were indexed using CrysAlis[1] software to obtain the unit cell parameters. The structures were solved with the direct methods (SHELXS-97) and refined on F^2 by full-matrix least-squares (SHELXL-97).[2]

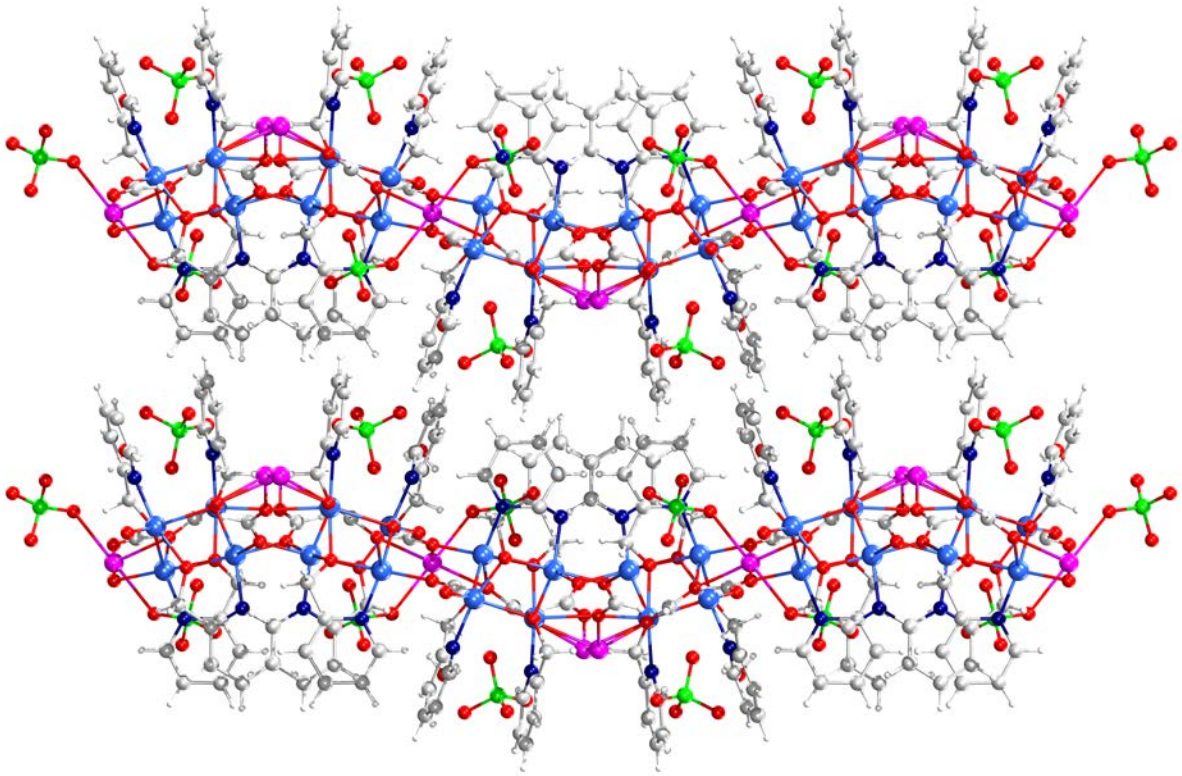

Fig. S1. The 3D structure of **1** viewed along crystallographic *a* axis.

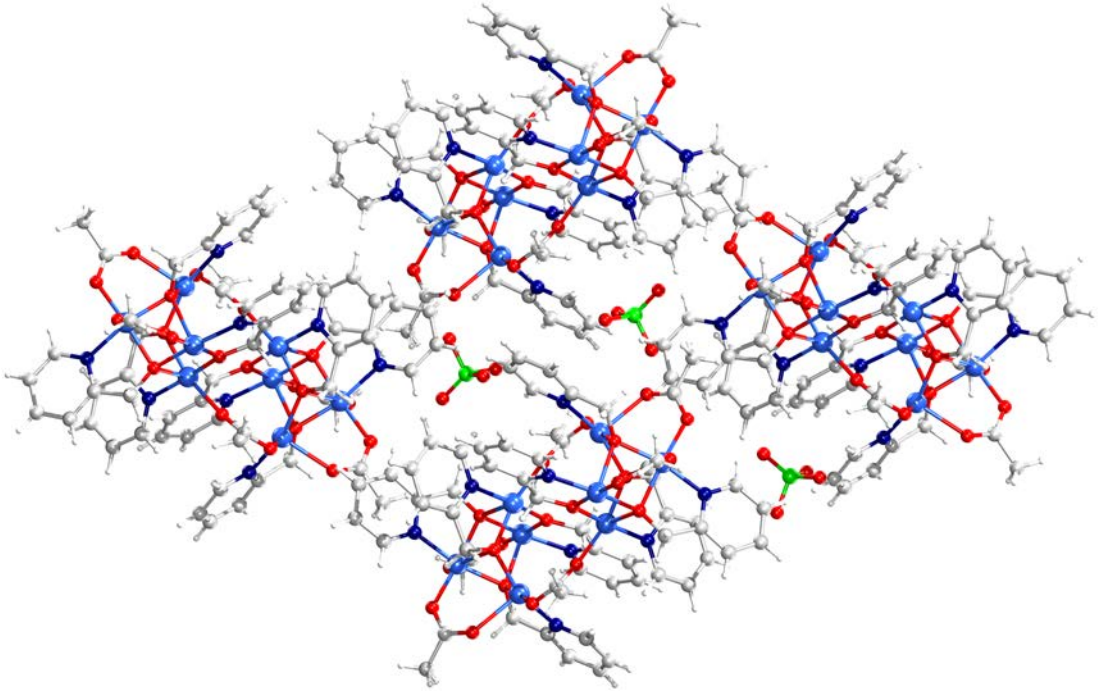

Fig. S2. The packing structure of **2** viewed along crystallographic *a* axis (C, gray; N, dark blue; O, red; Cu, light blue; H, white; Cl, green).

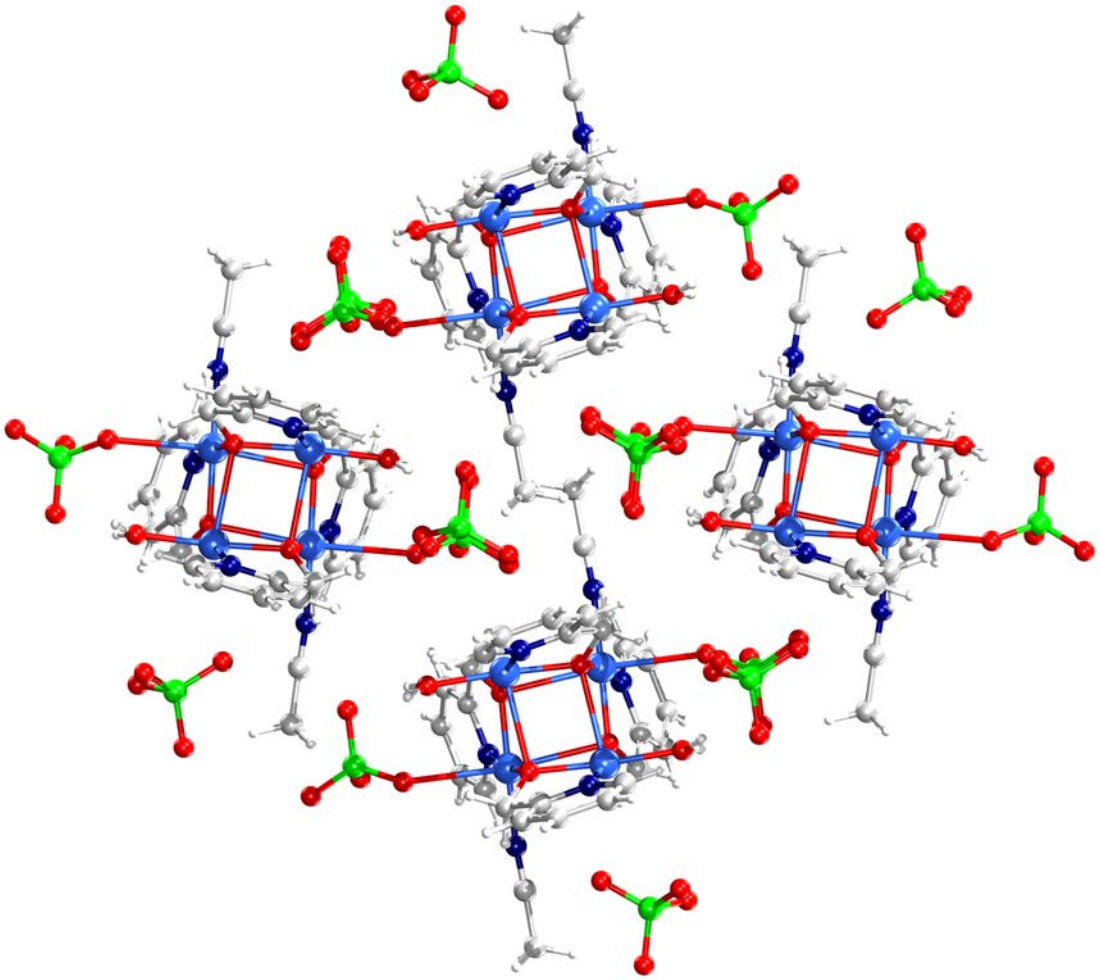

Fig. S3. The packing structure of **3** viewed along crystallographic *c* axis (C, gray; N, dark blue; O, red; Cu, light blue; H, white; Cl, green).

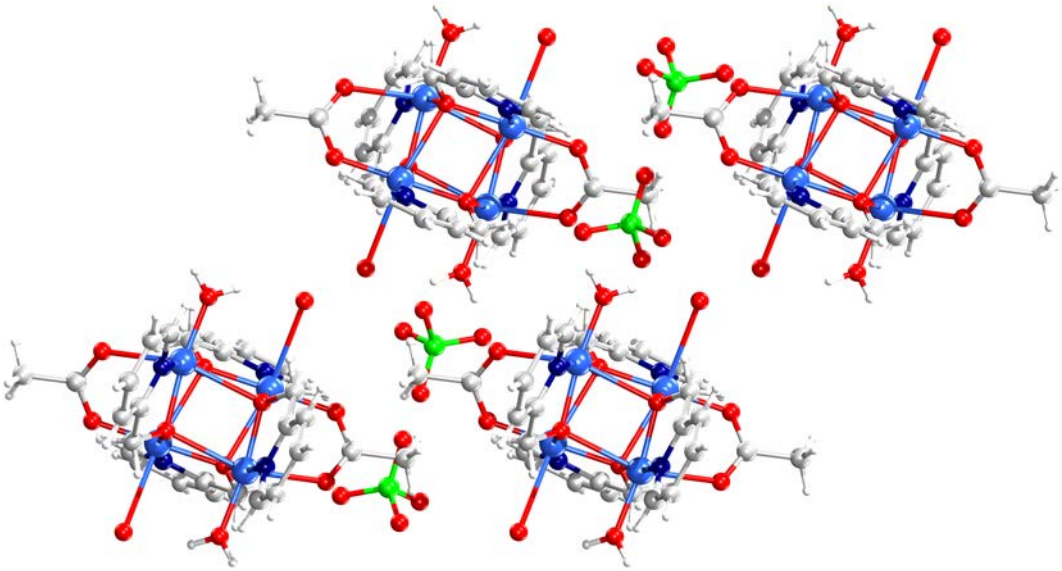

Fig. S4. The packing structure of **4** viewed along crystallographic *b* axis (C, gray; N, dark blue; O, red; Cu, light blue; H, white; Cl, green).

2.1 Table S1. Selected bond distances (Å) for complexes 1-4. (#1: 2-x, -y, z and #2: –x, y, 0.5-z)

1		**2**		**3**		**4**	
Cu(1)-O(1)	1.949(5)	Cu(1)-O(1)	1.970(4)	Cu(1)-O(1)	1.901(6)	Cu(1)-O(1)	1.944(3)
Cu(1)-O(4)	1.933(5)	Cu(1)-O(4)	1.944(4)	Cu(2)-O(1)	1.941(6)	Cu(1)-O(2)	1.941(3)
Cu(2)-O(3)	1.958(5)	Cu(2)-O(3)	1.948(4)	Cu(2)-O(2)	1.903(6)	Cu(1)-O(1)#2	2.468(3)
Cu(2)-O(2)	1.909(5)	Cu(2)-O(2)	1.928(4)	Cu(1)#1-O(2)	1.963(5)	Cu(2)-O(2)	1.968(3)
Cu(3)-O(1)	1.950(5)	Cu(3)-O(1)	1.959(4)	Cu(1)#1-O(1)#1	1.901(6)	Cu(2)-O(1)#2	1.949(3)
Cu(3)-O(3)	2.002(5)	Cu(3)-O(3)	2.014(4)	Cu(2)#1-O(1)#1	1.941(5)	Cu(2)-O(2)#2	2.472(4)
Cu(4)-O(2)	1.912(5)	Cu(4)-O(2)	1.912(4)	Cu(1)-O(2)#1	1.963(6)	Cu(1)#2-O(1)	2.468(3)
Cu(4)-O(4)	1.975(6)	Cu(4)-O(4)	1.951(4)	Cu(2)#1-O(2)#1	1.903(6)	Cu(1)#2-O(1)#2	1.944(3)
Cu(2)-O(1)	2.485(5)	Cu(2)-O(1)	2.317(4)	Cu(1)-O(1)#1	2.573(5)	Cu(1)#2-O(2)#2	1.941(3)
Cu(3)-O(4)	2.489(5)	Cu(3)-O(4)	2.655(4)	Cu(1)#1-O(1)	2.573(5)	Cu(2)#2-O(1)	1.949(3)
Cu(4)-O(3)	2.351(5)	Cu(4)-O(3)	2.390(4)	Cu(2)#1-O(2)	2.544(5)	Cu(2)#2-O(2)	2.472(4)

2.2 Table S2. Selected bond angles (°) for complexes 1-4.

1		2		3		4	
Cu(1)-O(1)-Cu(2)	121.64(22)	Cu(1)-O(1)-Cu(2)	120.47(17)	Cu(1)-O(1)-Cu(2)	110.19(29)	Cu(1)-O(1)#2-Cu(2)	85.46(10)
Cu(1)-O(2)-Cu(2)		Cu(1)-O(2)-Cu(2)		Cu(1)-O(2)#1-Cu(2)	87.74(17)	Cu(1)-O(2)-Cu(2)	101.24(12)
Cu(1)-O(1)-Cu(3)	102.36(22)	Cu(1)-O(1)-Cu(3)	104.33(18)	Cu(1)#1-O(1)#1-Cu(2)#1	110.19(29)	Cu(1)#2-O(1)-Cu(2)#2	85.46(10)
Cu(1)-O(4)-Cu(3)	85.81(18)	Cu(1)-O(4)-Cu(3)	83.32(13)	Cu(1)#1-O(2)-Cu(2)#1	87.74(17)	Cu(1)#2-O(2)#2-Cu(2)#2	101.24(12)
Cu(1)-O(2)-Cu(4)		Cu(1)-O(2)-Cu(4)		Cu(1)-O(2)#1-Cu(2)#1	109.88(27)	Cu(1)-O(1)-Cu(2)#2	108.42(15)
Cu(1)-O(4)-Cu(4)	121.01(25)	Cu(1)-O(4)-Cu(4)	120.62(19)	Cu(1)-O(1)#1-Cu(2)#1	87.90(19)	Cu(1)-O(2)-Cu(2)#2	90.57(12)
Cu(2)-O(1)-Cu(3)	84.36(18)	Cu(2)-O(1)-Cu(3)	86.64(14)	Cu(1)#1-O(2)-Cu(2)	109.88(27)	Cu(1)#2-O(1)#2-Cu(2)	108.42(15)
Cu(2)-O(3)-Cu(3)	98.67(22)	Cu(2)-O(3)-Cu(3)	96.02(16)	Cu(1)#1-O(1)-Cu(2)	87.90(19)	Cu(1)#2-O(2)#2-Cu(2)	90.57(12)
Cu(2)-O(2)-Cu(4)	109.60(24)	Cu(2)-O(2)-Cu(4)	111.02(24)	Cu(1)-O(1)-Cu(1)#1	98.12(24)	Cu(1)-O(1)-Cu(1)#2	102.47(14)
Cu(2)-O(3)-Cu(4)	92.42(19)	Cu(2)-O(3)-Cu(4)	93.11(14)	Cu(1)-O(1)#1-Cu(1)#1	98.12(24)	Cu(1)-O(1)#2-Cu(1)#2	102.47(14)
Cu(3)-O(3)-Cu(4)	102.92(20)	Cu(3)-O(3)-Cu(4)	105.31(16)	Cu(2)-O(2)#1-Cu(2)#1	97.39(20)	Cu(2)-O(2)-Cu(2)#2	103.13(12)
Cu(3)-O(4)-Cu(4)	98.95(19)	Cu(3)-O(4)-Cu(4)	98.07(15)	Cu(2)-O(2)-Cu(2)#1	97.39(20)	Cu(2)-O(2)#2-Cu(2)#2	103.13(12)

3. Equation 1. Theoretical expression for χ_m derived from van Vleck equation with the simplified Heisenberg Hamiltonian. The equation (1) is used for the analysis of complexes **3** and **4**, respectively.

The coupling scheme of copper centers for compound **3** and **4**:

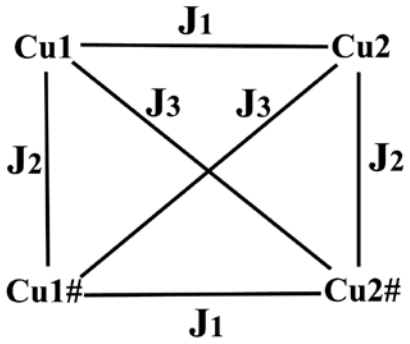

χ_m = (0.75/x)×p1×p1×[5×exp((p2+p3+p4)/x)+exp((p2-p3-p4)/x)+exp((-p2+p3-p4)/x)+exp(

(-p2-p3+p4)/x)]/[5×exp((p2+p3+p4)/x)+3×exp((p2-p3-p4)/x)+3×exp((-p2+p3-p4)/x)+3×exp(

(-p2-p3+p4)/x)+exp((-p2-p3-p4+2×((p2×p2+p3×p3+p4×p4-p2×p3-p2×p4-p3×p4)^0.5))/x)+

exp((-p2-p3-p4-2×((p2×p2+p3×p3+p4×p4-p2×p3-p2×p4-p3×p4)^0.5))/x)]+TIP (1)

P1---g; p2---J_1/k_B p3---J_2/k_B p4---J_3/k_B x---T

TIP---temperature independent paramagnetism

4. X-ray powder diffraction.

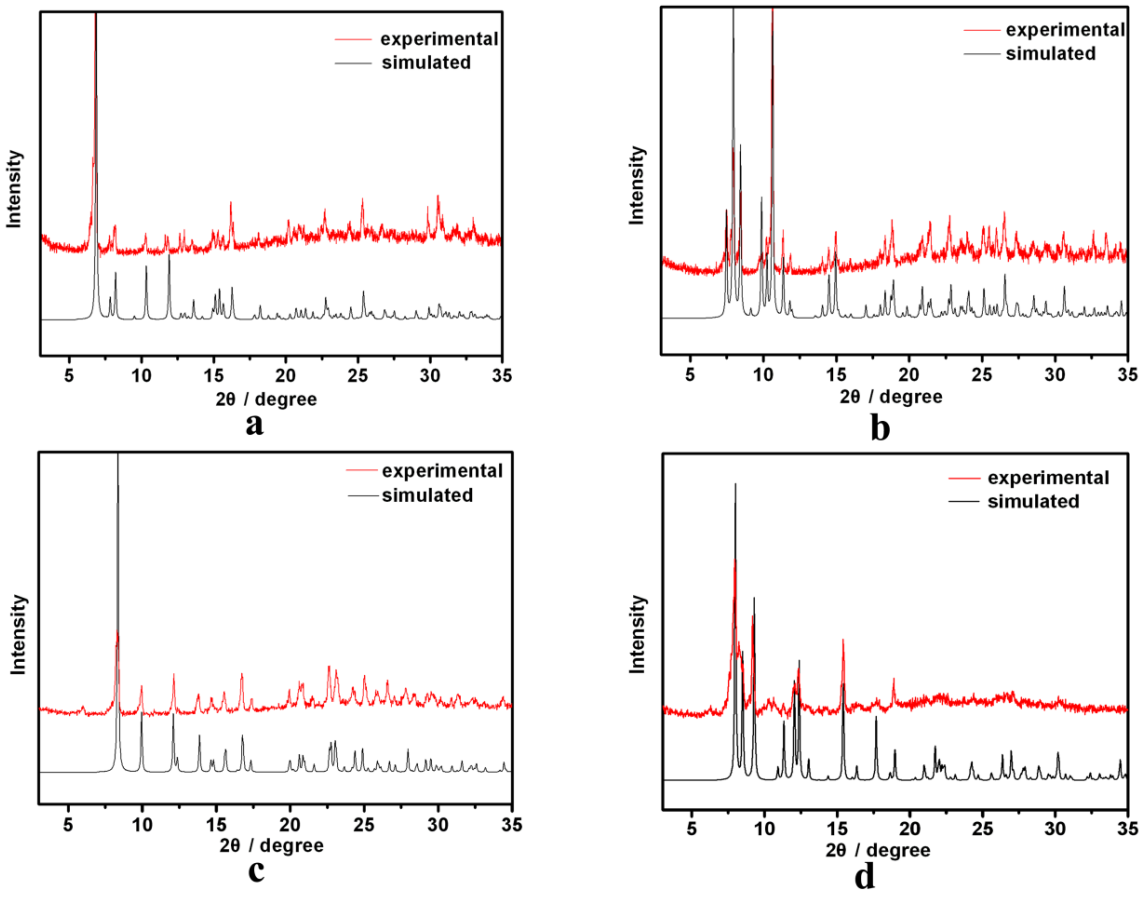

Fig. S5. X-ray powder diffraction patterns for (a) **1**, (b) **2**, (c) **3** and (d) **4**.

4. Magnetic studies.

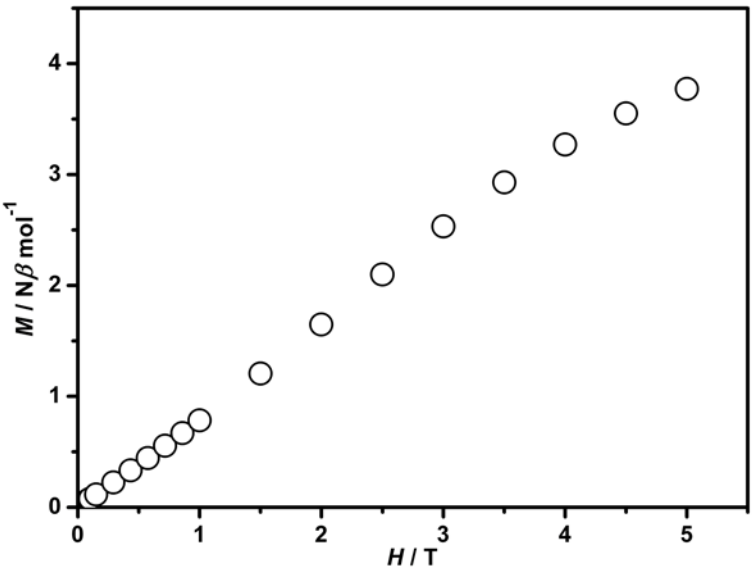

Fig. S6. Plot of $M/N\beta$ vs. H at 2 K for **1**.

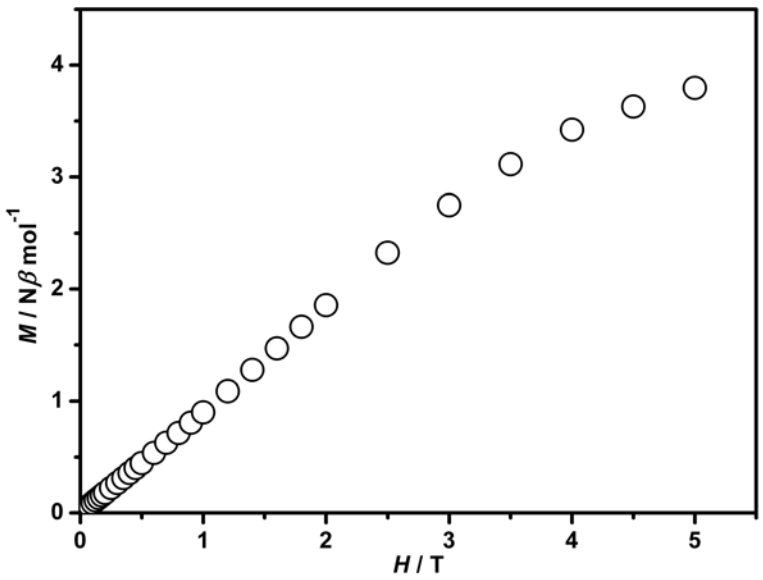

Figure S7. Plot of $M/N\beta$ vs. H at 2 K for **2**.

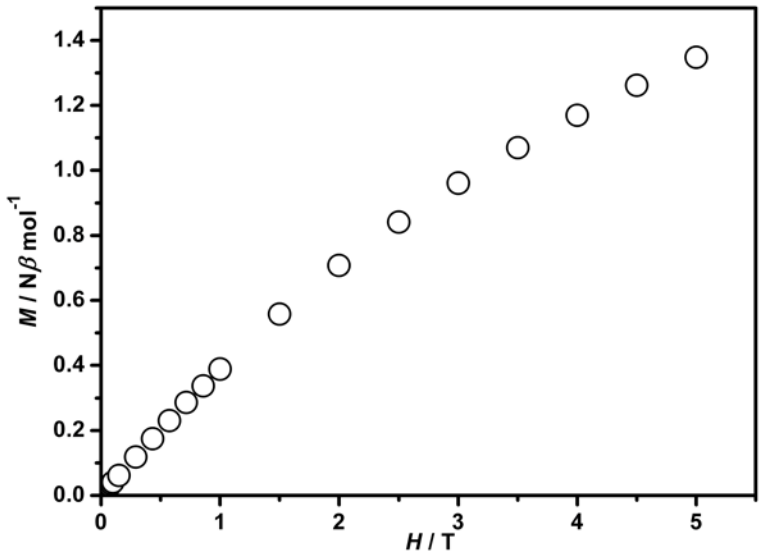

Figure S8. Plot of $M/N\beta$ vs. H at 2 K for **3**.

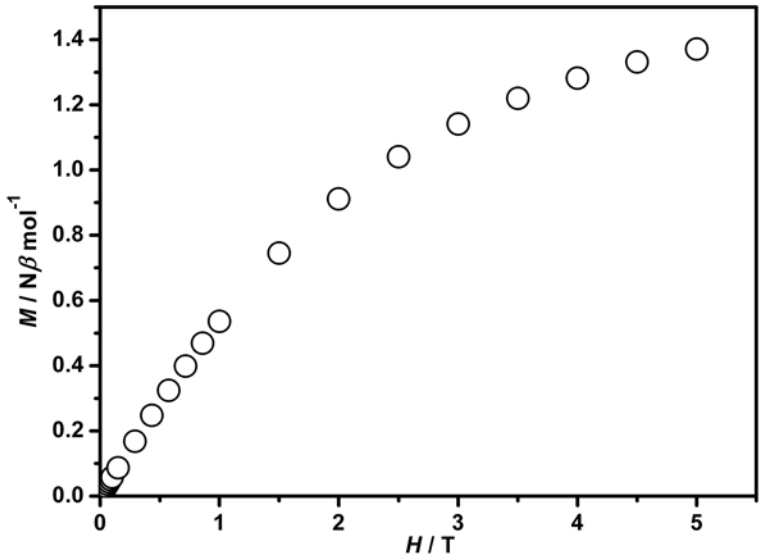

Figure S9. Plot of $M/N\beta$ vs. H at 2 K for **4**.

References:

1. Oxford Diffraction (2006). *CrysAlis*. Oxford Diffraction Ltd, Abingdon, Oxford, England.
2. (a) G. M. Sheldrick, *SHELXS97* and *SHELXL97*; University of Göttingen: Germany, 1997; (b) (b) G. M. Sheldrick, *Acta Crystallogr. Sect. A*: *Found. Crystallogr.*, 2008, **64**, 112-122.